

# Range Image Registration of Specular Objects under Complex Illumination

Diego Thomas  
National Institute of Informatics  
Tokyo 101-8430, Japan  
diego.thomas@nii.ac.jp

Akihiro Sugimoto  
National Institute of Informatics  
Tokyo 101-8430, Japan  
sugimoto@nii.ac.jp

## Abstract

*We present a method for range image registration of specular objects devoid of salient geometric properties under complex lighting environment. Our method uses illumination consistency on two range images to detect specular highlights, which are used to obtain diffuse reflection components. By using light information estimated from the specular highlights and the diffuse reflection components, we extract albedo at the surface of an object, even under unknown complex lighting environment. We then robustly register the two range images using extracted albedo. This technique can handle various kind of illumination situations and can be applied to a wide range of materials. Our experiments using synthetic data and real data show the effectiveness, the robustness and the accuracy of our proposed method.*

## 1. Introduction

Detailed modeling of real objects in controlled or uncontrolled environments has been of wide interest in the past decade. When creating the 3D model of a real object using laser range scanners, multiple range images of the same object are captured in different poses from a fixed viewpoint. Because each range image is represented in the local coordinate system depending on the position and pose of the sensor, the transformations aligning all images have to be computed. This process is called range image registration. The latest laser scanning technologies enable the accurate acquisition of both geometry and color information of the object of interest.

In this paper we will focus on range image registration of a non-Lambertian textured object devoid of salient geometric features under uncontrolled environment. We assume that two range images together with color images in different poses are captured from a fixed viewpoint under fixed unknown illumination conditions. We also assume that neither shadows nor inter-reflections exist.

The irradiance at a point on an object surface changes

when the object pose changes. As a consequence, the photometric appearance, such as color, of the same point in different range images changes. Using photometric features that depend on the object pose thus degrades the performance of the registration when they are used for establishing matching.

Albedo is the ratio of the diffuse reflected light over the irradiance, and it is invariant to the object pose, viewpoint or illumination condition. This property depends on only the object material and exhibits sufficient saliency for matching in the case of textured surfaces. Therefore, albedo is a powerful feature for range image registration of textured objects devoid of salient geometric features under fixed illumination conditions.

Albedo at a point can be directly computed when both the diffuse reflection and the incident illumination at this point are known. However, under uncontrolled environments or if the surface exhibits specular reflections (like shiny surfaces for example), computing albedo becomes a demanding problem. As a consequence, previous work that makes use of albedo, for example [3, 15], assumes the Lambertian surface (diffuse reflection only) and known incident illumination. In these approaches, specular reflections at the surface of an object are not considered.

We propose a method for registering two range images of a specular object under unknown illumination environment. To compute albedo at the surface, incident illumination and diffuse reflection components are required. For each range image, we generate candidates of light source directions, using normals at the surface and local peak of intensity. Illumination consistency on two range images allows us to detect incident illumination directions among the candidates. The detected incident illumination directions then enable us to define regions where the diffuse reflection components are accurately extracted. We compute albedo in these regions and extrapolate it by using neighboring similarities. In this way, we obtain albedo over the range images. The estimated albedo is used as an input of an existing registration algorithm to show the usefulness of our proposed method. Fig. 1 illustrates the flowchart of our

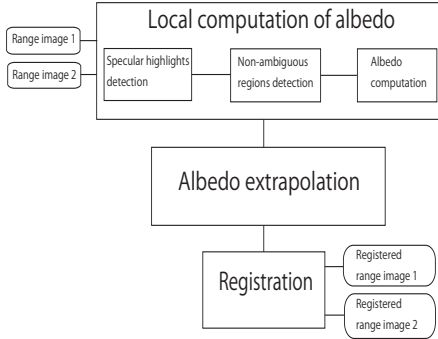


Figure 1: Basic flow of the proposed method.

proposed method. Our intensive experiments show the effectiveness of our proposed method. To our best knowledge, no method on range image registration has been proposed that can handle specular objects under unknown illumination environment.

## 2. Related work

For objects lacking in salient geometric features, many approaches using photometric features have been discussed. For example, Godin *et al.* [4] proposed to use dense attributes of range image elements as a matching constraint. Weik [17] proposed to use texture intensity gradient and intensity difference. Johnson and Kang [5] proposed to deal with textured 3D shapes by using color. Okatani *et al.* [10] proposed to use chromaticity for registration. Brusco *et al.* [2] proposed to incorporate texture information in the concept of spin-images. Pulli *et al.* [11] proposed a new mismatch error to improve registration using both color and geometric information. However, because color or chromaticity depends on the object pose, the viewpoint and illumination, the performance of these methods is degraded when the illumination change has significant effects on the object appearance.

On the other hand, albedo is a photometric property invariant to the pose of the object, the illumination condition and the viewpoint, and is thus powerful for the purpose of matching. Cerman *et al.* [3] proposed to use albedo difference to match points for range image registration. However, this point-based approach is sensitive to data noise and requires precise knowledge on the illumination. Therefore it is not practically applicable to real data.

More recently Thomas *et al.* [15] proposed to use local distribution of albedo to enhance robustness for range image registration. Adaptive regions are defined at the surface of an object by using local distribution of albedo and a metric is then defined to match points using the regions. The rigidity constraint on surface is also introduced to eliminate

false matches to improve accuracy of matching. Though this method achieves robust registration under a rough estimation of illumination, it is limited to Lambertian objects illuminated by a single distant light source.

In other approaches, Bay *et al.* [1] proposed a scale and rotation invariant descriptor called SURF that makes use of an integral image to speed up the computation and comparisons. Tola *et al.* [16] also proposed a local descriptor that can be quickly computed and used even in low-quality images. However, these techniques do not directly use available 3D information but use 2D information projected from 3D, and are thus sensitive to texture deformation caused by the projection. In fact, the same texture captured from different viewpoints produces differently deformed 2D textures, which makes these techniques problematic. Moreover, these approaches focus more on computational efficiency than on accuracy.

To deal with specular reflections under complex illumination environments, recent works on reflectance analysis can be used. Several methods to separate or decompose reflection components of textured surfaces can be found in the literature ([8], [12], [6]). For example, Lin *et al.* [6] proposed to separate reflection components from a sequence of images by computing the median intensity of corresponding pixels in the image sequence. However, this method requires a large number of images as well as pixel correspondences over all images. It is thus inappropriate for range image registration.

Tan *et al.* [13] proposed a method to separate reflection components of textured surfaces from a single image. By assuming the dichromatic reflection and a single distant light source, a specular free image is generated by locally and non-linearly shifting each pixel’s intensity and maximum chromaticity. This specular free image has exactly the same geometrical profile as the diffuse components. Though this method achieves accurate separation of reflection components, it can not handle multiple light sources and high intensity textures.

In contrast to previous work, our proposed method can handle changes in photometric appearance, non-Lambertian surfaces and unknown complex illumination environments even in the presence of high intensity textures.

## 3. Local computation of albedo

Computing albedo at the surface requires diffuse reflection components and light source directions. In the case of a scene illuminated by a single distant light source and given the corresponding illumination chromaticity, a method exists that separates the reflection components of the textured surface [13]. On the other hand, in our case, the illumination environment is not restricted to a single light source and such a separation technique can not be applied to the whole surface. However, even in the case of multiple light

sources, there exist some regions where the incident illumination can be approximated by a single light source. We thus divide the whole image into regions so that we have a region that is approximated by a single light source illumination. We call such regions non-ambiguous. We can then separate the reflection components of non-ambiguous regions to locally compute albedo.

### 3.1. Detection of specular highlights

For a smooth surface without high intensity texture, a specular highlight is centered on the mirror-like reflection direction, which is useful to estimate incident illumination direction. If the surface exhibits regions with high intensity texture, however, it becomes difficult to distinguish between specular highlights and regions with high intensity texture. Therefore, we first detect all highlights at the surface that can be either a specular highlight or a high intensity texture region. We then employ illumination consistency between two range images to discriminate specular highlights from high intensity texture regions.

**Highlight detection** If we consider a region with homogeneous texture, then a specular highlight will exhibit a local peak of intensity. This is because the specular reflection component increases as the viewing direction comes closer to the mirror-like reflection direction. We thus detect local peaks of intensities at the surface.

Points with lowest intensities in the image are first removed to focus on only significant specular highlights (with sufficient intensity). Then we obtain several connected regions. For each connected region, the average *avg* and standard deviation *std* of the intensities are computed, and each pixel  $\mathbf{x}$  such that  $\mathbf{I}(\mathbf{x}) > avg + std$  is selected, where  $\mathbf{I}(\mathbf{x})$  is the intensity at  $\mathbf{x}$ . Then, if the current connected region is separated into several connected parts, the same process is applied to each connected part. The detection stops when the number of connected regions becomes stable. Each connected region represents one possible specular highlight.

**Specular highlights** Some of the detected highlights may be high intensity texture regions, which may cause inaccurate estimation of incident illumination directions. We first compute light source direction of each highlight and then employ illumination consistency to discriminate between specular highlights and high intensity texture regions.

The illumination condition is assumed to be fixed when two range images are captured. This means that the light source directions producing corresponding specular highlights are the same in two range images. We will call this illumination consistency.

Normals at the surface are available for two range images. We can thus estimate the incident illumination direction that can produce such highlight. To be more specific,

we first compute the average of the incident light vectors in the highlight region, where an incident light vector at a point  $\mathbf{x}$  is computed by rotating the viewing directions at a point  $\mathbf{x}$  around the normal at point  $\mathbf{x}$  with an angle of  $\frac{\pi}{2}$ . This is because for smooth surfaces, the viewing directions in this region is roughly centered on the mirror-like specular reflection direction.

The highlight regions are then clustered into groups that are produced by similar light sources. Namely, consider the sets  $(H_{1,j})_{j \in [0, n_1]}$  and  $(H_{2,j})_{j \in [0, n_2]}$  of the highlight regions of two range images, with  $n_1$  and  $n_2$  the number of highlight regions. We combine highlight regions using the criterion below:

$$\forall i \in [1, 2], \forall (j, j') \in [0, n_i], \text{ if } \text{acos}(\mathbf{l}_{i,j} \cdot \mathbf{l}_{i,j'}) < Th_l$$

then the corresponding regions are combined,

(1)

where  $\mathbf{l}_{i,j}$  is the estimated normalized light direction for the highlight region  $H_{i,j}$ ,  $(\mathbf{l} \cdot \mathbf{l}')$  is the scalar product of two vectors  $\mathbf{l}$  and  $\mathbf{l}'$ , and  $Th_l$  is a threshold (for example 20 degrees). When two regions  $H_{i,j}$  and  $H_{i,j'}$  are combined into a group,  $H_{i,j'}$  is added to  $H_{i,j}$ ,  $l_{i,j} = \frac{l_{i,j} + l_{i,j'}}{2}$  and  $H_{i,j'}$  is removed from the list of highlight regions.

We then eliminate high intensity texture regions using the illumination consistency constraint. We here assume that for each range image, each light source illuminating the object produces specular reflections. This means that the distribution of normals at the surface should be wide enough, so that for each light source there exists at least one region at the surface for which the viewing direction is close to the mirror-like reflection direction.

Assume a region as a specular highlight in a range image and consider its corresponding light source direction. If no specular highlights can be found in the other range image with its similar corresponding light source direction, then the same light source does not illuminate the object in the other range image, which contradicts to the assumption of fixed illumination. Accordingly, we use the criterion below:

$$\forall i \in [1, 2], \forall j \in [0, n_i],$$

$$\text{if for } i' \in [1, 2], i' \neq i, \forall j' \in [0, n_{i'}],$$

$$\text{acos}(\mathbf{l}_{i,j} \cdot \mathbf{l}_{i',j'}) > Th_l,$$

then the region  $H_{i,j}$  is eliminated.

(2)

Fig. 2 illustrates the illumination consistency constraint under a fixed viewpoint and fixed illumination condition.

We finally obtain consistent specular highlights on two range images with their estimated incident light direction. These specular highlights are then used to compute the illumination chromaticity of each light source. The estimated light source direction are used to detect non-ambiguous regions each of which is mostly illuminated by a single dom-

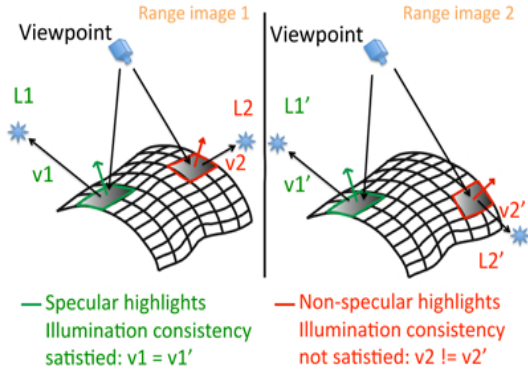


Figure 2: Illumination consistency constraint.

inant light source. Details of these procedures are given in the next sections.

### 3.2. Detection of non-ambiguous regions

For each specular highlight, we have estimated its mostly dominant light source direction. If the incident illumination of a region is a single distant light source, we can use the method [13]. We can not, however, directly apply the method [13] to the whole surface, because the illumination environment can be composed of multiple light sources. In fact, the method [13] requires a normalized image that simulates pure white illumination. However, we can not obtain a normalized image if the scene is illuminated by unknown multiple light sources with different colors. This is because the normalization process is not additive, not even linear.

We assume that each detected light source is distant from the surface so that the incident light rays coming from one light source is the same for all points at the surface. By using the detected incident light directions, we compute a shadow map for each detected light source. Namely, for a light  $L$  with its directional vector  $\mathbf{l} = (l_x, l_y, l_z)$ , we define the shadow map  $S$  induced by  $L$  proportional to the energy received from  $L$  by each point at the surface. More precisely, for a point  $\mathbf{x}$  on the surface with normal  $\mathbf{n}$  and with angle  $\Theta$  between  $\mathbf{l}$  and  $\mathbf{n}$ , we define

$$S(\mathbf{x}, L) = \cos\Theta. \quad (3)$$

To detect non-ambiguous regions, we use the criterion below:

$$\begin{aligned} &\text{if } (S(\mathbf{x}, L_1) \leq Th_\alpha \text{ or } S(\mathbf{x}, L_2) \leq Th_\alpha) \\ &\quad \text{then } \mathbf{x} \text{ is in a non-ambiguous region} \\ &\quad \text{else } \mathbf{x} \text{ is in an ambiguous region,} \end{aligned} \quad (4)$$

where  $L_1$  and  $L_2$  are the two light sources such that the intensity of the shadow maps at the point  $\mathbf{x}$  are greatest. The threshold  $Th_\alpha$  is a value between 0 and 1. In the experiments, we chose  $Th_\alpha = 0.7$  that corresponds to an angle

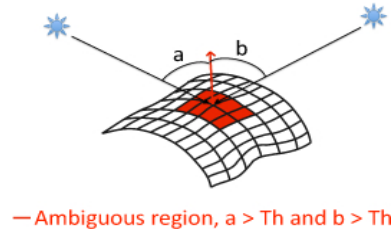


Figure 3: Definition of ambiguous regions.

$\Theta$  of about 45 degrees. For each non-ambiguous regions, we attach the light source that emits the most energy inside this region and regroup regions with the same corresponding light sources. We remark that it is preferable to over-detect ambiguous regions rather than non-ambiguous regions. This is because errors in the albedo estimation may propagate during the subsequent extrapolation process.

As a consequence, we obtain non-ambiguous regions in two range images in which we can reliably and adaptively separate reflection components using a single distant light source.

### 3.3. Estimating albedo of non-ambiguous regions

For each non-ambiguous region, the incident illumination can be approximated by a distant single light source whose illumination chromaticity can be estimated. We can thus independently apply the method proposed in [13] to each non-ambiguous regions for separating reflection components of these parts of the surface. We briefly recall the method proposed in [13].

The dichromatic reflection model at a pixel  $\mathbf{x}$  can be expressed as:

$$\mathbf{I}(\mathbf{x}) = \omega_d(\mathbf{x})\mathbf{B}(\mathbf{x}) + \omega_s(\mathbf{x})\mathbf{G}(\mathbf{x}), \quad (5)$$

where  $\mathbf{I} = (I_r, I_g, I_b)$  is the color vector of image intensity,  $\mathbf{x} = (x, y)$  is the image coordinates,  $\omega_d(\mathbf{x})$  and  $\omega_s(\mathbf{x})$  are the weighting factors for diffuse and specular reflections,  $\mathbf{B}(\mathbf{x})$  represents the color vector of the diffuse reflection and  $\mathbf{G}(\mathbf{x})$  represents the color vector of the specular reflection. Note that we assume that the specular reflection intensity is equal to the illumination intensity, without any inter-reflections. The first part of the right-hand side in (5) represents the diffuse reflection component and the second part represents the specular reflection component. The basic idea for separating reflection components is to iteratively compare the intensity logarithmic differentiation of an input image and its specular-free image. We remark that a specular-free image is an image that has exactly the same profile as the diffuse image.

The input image should be a normalized image that simulates a pure white illumination. Accordingly, the input image is normalized by the illumination chromaticity. To

compute illumination chromaticity, several methods based on color constancy can be found in the literature. In particular, the method [14] achieves robustness as well as accurate estimation of the illumination chromaticity by using specular reflection intensity. The specular-free image is generated by shifting each pixel’s intensity and maximum chromaticity nonlinearly. Given a normalized and a specular-free image, the reflection components are then iteratively separated until the normalized image has only diffuse pixels.

As a result, a diffuse normalized image is obtained. This estimated diffuse image is then used, together with the estimated light source direction corresponding to the non-ambiguous region and the diffuse reflection model, to estimate albedo in this region.

#### 4. Extrapolating albedo into ambiguous regions

Up to here, we have computed albedo in non-ambiguous regions. However, in ambiguous regions, albedo is still unknown and matching points in these regions is not yet possible. We remark that albedo has been computed in several parts in the surface and we expect that several points in the ambiguous regions have albedo similar to points in non-ambiguous regions. We thus estimate albedo in the ambiguous region by extrapolating albedo computed in non-ambiguous regions.

We consider a small region at the surface without specular highlights. The energy reflected at points inside this region is then mostly diffuse. As a consequence, the chromaticity or maximum chromaticity of points inside this region with the same surface color is similar to each other. Therefore, by comparing maximum chromaticity of points inside the regions, we can identify points having similar albedo.

For a point  $\mathbf{x}$  at the surface, the maximum chromaticity  $\sigma(\mathbf{x})$  of the point  $\mathbf{x}$  is defined as follows:

$$\sigma(\mathbf{x}) = \frac{\max(I_r(\mathbf{x}), I_g(\mathbf{x}), I_b(\mathbf{x}))}{I_r(\mathbf{x}) + I_g(\mathbf{x}) + I_b(\mathbf{x})}. \quad (6)$$

Starting from the diffuse points in the ambiguous region that have a neighbor in a non-ambiguous region, albedo values are iteratively and locally extrapolated until the size of the ambiguous region converges to a constant value. At each iteration, considering a point  $\mathbf{x}$  at the border of the ambiguous region, we extract the point  $\mathbf{y}$  in the neighborhood of  $\mathbf{x}$  such that  $\epsilon = |\sigma(\mathbf{x}) - \sigma(\mathbf{y})|$  is minimal and albedo of  $\mathbf{y}$  is known. If  $\epsilon$  is smaller than a threshold  $Th_\epsilon$  (for example  $Th_\epsilon = 0.1$ ), then we set the albedo value of  $\mathbf{x}$  to the one of  $\mathbf{y}$  and remove  $\mathbf{x}$  from the ambiguous region. Namely, we

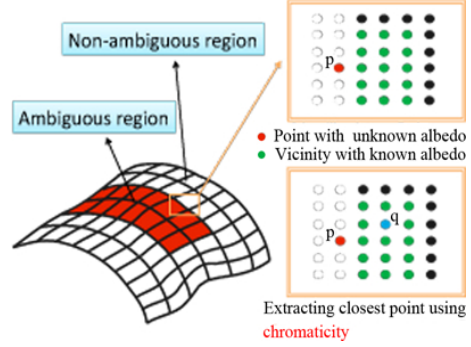


Figure 4: Albedo extrapolation.

process as follows:

$$\begin{aligned} \mathbf{y} = \operatorname{argmin}_{\mathbf{p} \in V(\mathbf{x})} (|\sigma(\mathbf{x}) - \sigma(\mathbf{p})|), \\ \text{if } |\sigma(\mathbf{x}) - \sigma(\mathbf{y})| < Th_\epsilon, \\ \text{then } alb(\mathbf{x}) = alb(\mathbf{y}) \end{aligned} \quad (7)$$

and we remove  $\mathbf{x}$  from the ambiguous region,

where  $alb(\mathbf{x})$  is the albedo of point  $\mathbf{x}$  and  $V(\mathbf{x})$  is a neighborhood of  $\mathbf{x}$  such that  $\forall \mathbf{p} \in V(\mathbf{x}), \|\mathbf{x} - \mathbf{p}\|_2 < Th_V$  and  $\mathbf{p}$  is in a non-ambiguous region, with  $Th_V$  a threshold (for example  $Th_V = 0.06$  mm if the resolution of range image is 0.01 mm). Fig. 4 illustrates different stages of the extrapolation procedure.

As a result, we extrapolate albedo to the rest of points on the surface that are not inside a specular highlight. We then obtain albedo over the surface. The estimated albedo thus becomes useful for registering range images. The obtained range image where each point has its corresponding albedo is called the albedo map.

#### 5. Registration

In order to show the usefulness of our method, we use our estimated albedo map as an input of the iterative method for range image registration proposed in [15].

The method [15] uses adaptive regions defined from the local distribution of albedo. Namely, by defining a speed image for a range image, a contour is propagated from each point using a level-set approach, which defines an adapted region for each point.

A similarity metric between two points of interest is then defined based on supports from the corresponding points inside regions for the two points. This similarity metric represents the albedo similarity of corresponding points inside the regions weighted by the geometric similarity of the regions. To eliminate incorrect matches the rigidity constraint is used.

As a result, the obtained list of matches is robust and accurate enough to be used for the estimation of the transformation using a weighted least square approach [7].

## 6. Experiments

### 6.1. Evaluation with synthetic data

We conducted experiments with synthetic data to verify the robustness of our proposed method with respect to noise in both normals and intensity and against changes in illumination conditions. The synthetic data were obtained with a 3D modeler software (3D Studio Max) (see Table 1). The exact albedo image is known and intensity at the surface with a known specular reflection component and synthetic light sources was simulated using the Torrance and Sparrow reflection model [9] (Fig. 5).

Before applying our method, we manually established a rough pre-alignment of two range images. This alignment allowed us to simulate the case where the input data were captured from two different viewpoints rotationally differentiated by 18.09 degrees around the axis (0.0057, 0.9997, -0.025).

In order to see the effects against data noise, we randomly transformed the normals and intensity of the two range images. More precisely, let the latitude and longitude angles in the unit sphere between the direction of a perturbed normal and a ground truth normal be  $\alpha$  and  $\Theta$  respectively, in which  $\Theta$  is uniformly generated from 0 degree to 360 degrees. The normals were perturbed with different values of  $\alpha$ . On the other hand, the surface intensity was perturbed with Gaussian noise with 0 mean and  $\lambda$  variance, where  $\lambda$  is a percentage of the average of the ground truth intensity of the surface.

We evaluated our method with different values of  $\alpha$  and  $\lambda$ . The value  $\alpha$  was changed from 0 to 10.3 degrees by 0.6 degrees. The value  $\lambda$  was changed from 0 to 8.5 percents by 0.5 percents. For each values of  $\alpha$ ,  $\lambda$ , we applied our method 20 times under the same initial conditions.

Figures 6 and 7 show quantitative evaluation of registration results in terms of averages and variances of the angle error and axis error of the obtained results under various different level of noise in normals and in intensity, respectively. We observe that even with a noise in normals of variance 10 degrees, the largest error remains under 0.2 degrees for the angle accuracy and under 1.0 degrees for the axis accuracy. For noise in intensity, we observe that even with a noise of variance 8%, the largest error remains under 0.8 degrees for the angle accuracy and under 2.5 degrees for the axis accuracy. Our method achieves robustness for both noise in normals and intensity.

Figure 8 shows the estimated albedo computed for the input range images in Fig. 5 and the qualitative result of the registration. We observe that as expected the specular effects are correctly removed and that the estimated albedo is globally invariant to the viewpoint, the pose of the object and the illumination. We also observe that the registration achieves accuracy with the same precision as the acquisition

Table 1: Description of the synthetic data.

Nb.Points	Resolution	Expected_rot (angle; axis)
30650	0.01mm	(18.090; 0.006, 0.999, -0.025)



Figure 5: The input synthetic data.

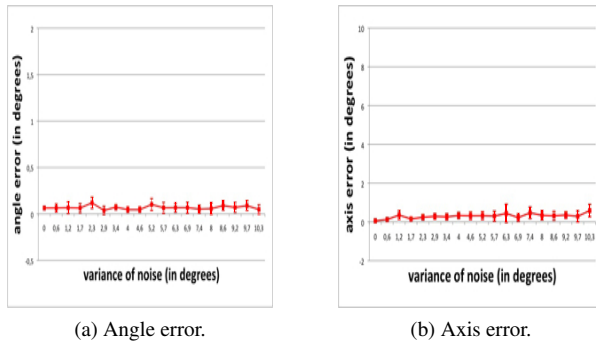


Figure 6: Results under noise in normals.

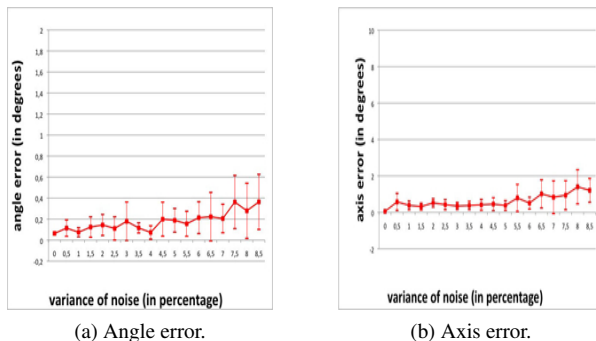


Figure 7: Results under noise in intensity.

device accuracy. The albedo maps are as expected consistent for the two range images.

In order to see the effects against illumination conditions, we rendered two images with various kinds of illumination. The light source direction is then computed using the normal at the point  $x$  and the viewpoint, and the light source position is defined with an arbitrary distance in the



Figure 8: Albedo map of input images and registration results.

light source direction. This is because we need specular highlights at the surface and we preferred to choose a random point  $x$  at the surface that represents the perfect specular reflection from the viewpoint rather than choosing the position of the light source randomly.

We changed the position between the specular highlights defining the light source directions. One light was fixed and considered as a reference light and we evaluated our method with three different value of  $d$ : 1.8, 1.2 and 0.8 where  $d$  is the distance of the two ideal reflection points. For each value of  $d$ , our method was applied 20 times with a random light direction.

Table 2 shows the results obtained with our method. The value *Ratio* is the ratio of ambiguous points over the total number of points in the two range images. We observe that the largest error remains under 1.0 degree for the angle accuracy and under 4 degrees for the axis accuracy. Figs. 9 and 10 illustrates the results obtained with our method when using two light sources with  $d = 1.2$ . We show for comparison, results obtained with the method proposed in [15]. We observe that the diffuse reflection model did not work at all. The result obtained with the method [15] has an angle error of 12.12 degrees and an axis error of 20.02 degrees. In contrast, our method obtained accurate result, with an angle error of 0.34 degrees and an axis error of 0.66 degrees. We observe that our method effectively extracts albedo over the range images. The ratio of ambiguous points was of 0.405 in this experiment.

## 6.2. Evaluation with real data

We also conducted experiments using a real object. We employed a Konica Minolta Vivid 910 range scanner to obtain two range images of a sphere (that we call data *globe*) with specular reflection components under fixed and uncontrolled illumination (Fig. 11). This sphere was with diameter of about 10cm. A mechanic system was used for rotations to obtain ground truth of transformation.

Figure 11 shows the input range images acquired under fixed and unknown illumination, from the same viewpoint and with two different poses. Table 3 show the details of the

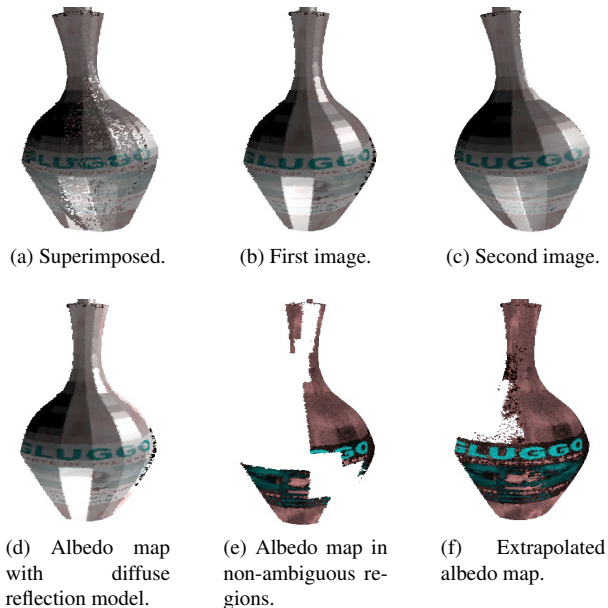


Figure 9: Simulation with two light sources.

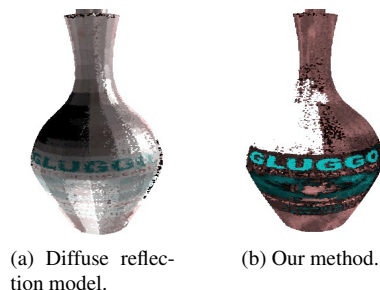


Figure 10: Obtained results

data *globe*. Fig. 12 shows the obtained albedo map and the qualitative registration result using the proposed method. From Fig. 12 (a) and (b), we observe that our method succeeded in extracting albedo even in the presence of specular highlights and high intensity textures. As expected, the specular reflections are successfully removed and the albedo maps are consistent over the two range images. Using our estimated albedo we could obtain accurate registration result (Fig. 12 (c)). The angle error of the registration was about 0.17 degrees and the axis error was about 0.79 degrees. The ratio of ambiguous points was about 0.12.

Table 3: Description of the data *globe*.

Nb_Points	Resolution	Expected_rot (angle; axis)
31000	0.53mm	(22.495; 0.025, 0.942, -0.334)

Table 2: Results obtained with two light sources.

$d$	Angle error	Variance of angle error	Axis error	Variance of axis error	Ratio	Variance of ratio
1.8	0.307 degrees	0.073 degrees	0.816 degrees	0.389 degrees	0.501	0.007
1.2	0.343 degrees	0.347 degrees	2.07 degrees	1.95 degrees	0.502	0.335
0.8	0.427 degrees	0.415 degrees	1.767 degrees	1.64 degrees	0.392	0.39

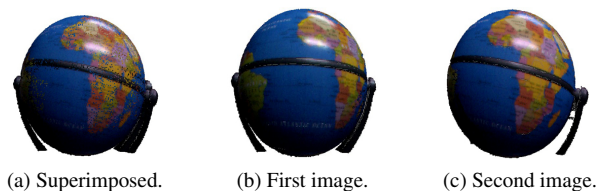


Figure 11: The input data *globe*.

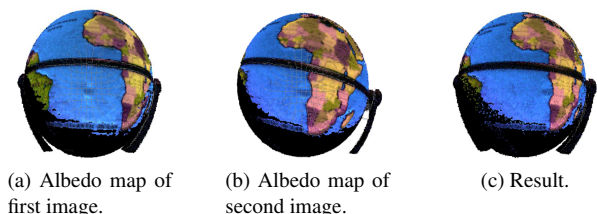


Figure 12: Results with data *globe*.

## 7. Conclusion

We proposed a method for the registration of range images of specular objects devoid of salient geometric features under uncontrolled illumination. By using highlights at the surface and illumination consistency on two range images, we estimate the incident illumination. We then use the illumination information and the dichromatic model of reflection in order to locally estimate albedo. Locally estimated albedo is then extrapolated into the whole surface to obtain reliable albedo map. A range image registration technique is then used to estimate the transformation aligning two range images. Experiments using synthetic data and real data confirm the robustness and the accuracy of our proposed method.

## Acknowledgements

The authors are thankful to Robby T. Tan for his insightful suggestion on this work. This work was in part supported by JST, CREST.

## References

- [1] H. Bay, A. Ess, T. Tuytelaars, and L. Gool. Speeded-up robust features (surf). *CVIU'08*, 110(3):346–359, 2008. 2
- [2] N. Brusco, M. Andreetto, A. Giorgi, and G. M. Cortelazzo. 3D registration by textured spin-images. *In Proc. of 3DIM'05*, pages 262–269, 2005. 2
- [3] L. Cerman, A. Sugimoto, and I. Shimizu. 3D shape registration with estimating illumination and photometric properties of a convex object. *In Proc. of CVWW'07*, pages 76–81, 2007. 1, 2
- [4] G. Godin, D. Laurendeau, and R. Bergevin. A method for the registration of attributed range images. *In Proc. of 3DIM'01*, pages 179–186, 2001. 2
- [5] A. E. Johnson and S. B. Kang. Registration and integration of textured 3D data. *Image and vision computing*, 17(2):135–147, 1999. 2
- [6] S. Lin, Y. Li, S. Kang, X. Tong, and H. Shum. Diffuse-specular separation and depth recovery from image sequences. *In Proc. of ECCV'02*, pages 210–224, 2002. 2
- [7] Y. Liu, h. Zhou, X. Su, M. Ni, and R. J.Lloyd. Transforming least squares to weighted least squares for accurate range image registration. *In Proc. of 3DPVT'06*, pages 232–239, 2006. 5
- [8] S. Nayar, X. Fang, and T. Boult. Separation of reflection components using color and polarization. *Int'l J. Computer Vision*, 21(3), 1996. 2
- [9] S. Nayar, K. Ikeuchi, and T. Kanade. Surface reflection: Physical and geometrical perspectives. *Trans on PAMI'91*, 13(7):611–634, 1991. 6
- [10] Okatani, I.S., and A. Sugimoto. Registration of range images that preserves local surface structures and color. *In Proc. of 3DPVT'04*, pages 786–796, 2004. 2
- [11] K. Pulli, S. Piironen, T. Duchamp, and W. Stuetzle. Projective surface matching of colored 3D scans. *In Proc. of 3DIM05*, pages 531–538, 2005. 2
- [12] Y. Sato and K. Ikeuchi. Temporal-color space analysis of reflection. *J. Optics Soc. Am. A*, 11, 1994. 2
- [13] R. Tan and K. Ikeuchi. Separating reflection components of textured surfaces using a single image. *IEEE Trans. on PAMI'05*, 27(2):178–193, 2005. 2, 4
- [14] R. Tan, K. Nishino, and K. Ikeuchi. Color constancy through inverse intensity chromaticity space. *J. Optics Soc. Am. A*, 21(3):321–334, 2004. 5
- [15] D. Thomas and A. Sugimoto. Robust range image registration using local distribution of albedo. *In Proc. of 3DIM'09*, pages 1654–1661, 2009. 1, 2, 5, 7
- [16] E. Tola, V. Lepetit, and P. Fua. A fast local descriptor for dense matching. *In Proc. of CVPR'08*, pages 1–8, 2008. 2
- [17] S. Weik. Registration of 3-D partial surface models using luminance and depth information. *In Proc. of 3DIM'97*, pages 93–101, 1997. 2